J|A|C|S
ARTICLES
Published on Web 03/09/2004

Electronic Structure and Solvation of Copper and Silver Ions: A Theoretical Picture of a Model Aqueous Redox Reaction

Jochen Blumberger,[†] Leonardo Bernasconi,[†] Ivano Tavernelli,[†,§] Rodolphe Vuilleumier,[‡] and Michiel Sprik*,[†]

Contribution from the Department of Chemistry, University of Cambridge, Cambridge CB2 1EW, United Kingdom, and Laboratoire de Physique Théorique des Liquides, Université P. et M. Curie, 4 Place Jussieu, 75005 Paris, France

Received October 15, 2003; E-mail: ms284@cam.ac.uk

Abstract: Electronic states and solvation of Cu and Ag aqua ions are investigated by comparing the $Cu^{2+} + e^- \rightarrow Cu^+$ and $Ag^{2+} + e^- \rightarrow Ag^+$ redox reactions using density functional-based computational methods. The coordination number of aqueous Cu^{2+} is found to fluctuate between 5 and 6 and reduces to 2 for Cu^+, which forms a tightly bound linear dihydrate. Reduction of Ag^{2+} changes the coordination number from 5 to 4. The energetics of the oxidation reactions is analyzed by comparing vertical ionization potentials, relaxation energies, and vertical electron affinities. The model is validated by a computation of the free energy of the full redox reaction $Ag^{2+} + Cu^+ \rightarrow Ag^+ + Cu^{2+}$. Investigation of the one-electron states shows that the redox active frontier orbitals are confined to the energy gap between occupied and empty states of the pure solvent and localized on the metal ion hydration complex. The effect of solvent fluctuations on the electronic states is highlighted in a computation of the UV absorption spectrum of Cu^+ and Ag^+.

Introduction

The differences between the chemistry of first and second row transition metals can be substantial. The aqua ions of the group IB elements Ag and Cu are a good example.[1] The redox potential for $Cu^{2+} + e^- \rightarrow Cu^+$ is only 0.15 V, and both oxidation states are observed. Indeed, Cu^{2+} is often featured as the classic example of a transition metal aqua ion with a six-fold octahedral hydration shell. Cu^+, in practice, can only be produced in vanishingly small concentration because of the instability against disproportionation ($2Cu^+ \rightarrow Cu^{2+} + Cu$). For silver, the stability is reversed. The $Ag^{2+} + e^- \rightarrow Ag^+$ electrode potential is as high as 2.0 V, making Ag^{2+} one of the most aggressive aqueous oxidants. Ag^+ is a poorly soluble but stable aqua ion.

Group IB ions also stand out because of their highly fluxional hydration shells. Exchange times for water molecules in the first hydration shell of Cu^{2+} are in the range of 200 ps, placing Cu^{2+} at the very fast end of the scale for ions of any charge[2] despite the huge hydration enthalpy of $\Delta H_{hydr} = 2100$ kJ mol^{-1}. For a comparison, Ni^{2+} has a very similar ionic radius and a hydration enthalpy of only 10 kJ/mol more, but the exchange times are 4 orders of magnitude slower. The hydration shell of Ag^+ is equally mobile, which has hampered experimental determination of its structure. The consensus is now that Ag^+ is coordinated by four H_2O molecules in an approximately tetrahedral configuration.[3−6] Ag^+ ions, however, are notorious for their structural flexibility, assuming a wide variety of coordination patterns in solid compounds. The energy differences between these structures are minimal, which is why some Ag^+ compounds are superionic conductors. Finally, while not stable in solution, the hydration of Cu^+ can be studied in the gas phase and also shows marked deviations from classical rigid ion behavior, as is manifested in a pronounced discontinuity in the stepwise formation constant of $Cu^+(H_2O)_n$ complexes when n is increased from 2 to 3.[7−11]

The complexity of the aqueous chemistry of IB metal ions is a consequence of their position at the close of the d block transition series. Cu^{2+} and Ag^{2+} have a d^9 configuration, and Cu^+ and Ag^+ are formally closed shell (d^{10}). This gives rise to a number of vibronic instabilities familiar from solid transition metal compounds.[12] In liquid solutions, the restrictions on the geometry of coordination shells are much less severe than those in solids, which may amplify some of these effects. As a result, the rearrangement of the hydration shell induced by vertical

† University of Cambridge.
‡ Université P. et M. Curie.
§ Present address: Institute of Molecular and Biological Chemistry, Federal Institute of Technology-EPFL, 1015 Lausanne, Switzerland.

(1) Greenwood, N. N.; Earnshaw, A. *Chemistry of the Elements*, 2nd ed.; Butterworth-Heinemann: Oxford, 1997.
(2) Cusanelli, A.; Frey, U.; Richens, D. T.; Merbach, A. E. *J. Am. Chem. Soc.* **1996**, *118*, 5265.
(3) Texter, J.; Hastreiter, J. J.; Hall, J. L. *J. Phys. Chem.* **1983**, *87*, 4690.
(4) Sandström, M.; Neilson, G. W.; Johansson, G.; Yamaguchi, T. *J. Phys. C: Solid State Phys.* **1985**, *18*, 1115.
(5) Skipper, N. T.; Neilson, G. W. *J. Phys.: Condens. Matter* **1989**, *1*, 4141.
(6) Ohtaki, H.; Radnai, T. *Chem. Rev.* **1993**, *93*, 1157.
(7) El-Nahas, A. M.; Hirao, K. *J. Mol. Struct. (THEOCHEM)* **1999**, *469*, 201.
(8) El-Nahas, A. M.; Hirao, K. *J. Phys. Chem. A* **2000**, *104*, 138.
(9) Feller, D.; Glendening, E. D.; de Jong, W. A. *J. Chem. Phys.* **1999**, *110*, 1475.
(10) Bauschlicher, C. W., Jr.; Langhoff, S. R.; Partridge, H. *J. Chem. Phys.* **1991**, *94*, 2068.
(11) Magnera, T. F.; David, D. E.; Stulik, D.; Orth, R. G.; Jonkmann, H. T.; Michl, J. *J. Am. Chem. Soc.* **1989**, *111*, 5036.
(12) Bersuker, I. B. *Electronic Structure and Properties of Transition Metal Compounds*; Wiley & Sons: New York, 1996.

 10.1021/ja0390754 CCC: $27.50

ionization can be rather drastic. This is one of the issues investigated in the numerical study reported here. The relaxation is studied from an electrochemical perspective, treating the $Cu^{2+} + e^- \rightarrow Cu^+$ and $Ag^{2+} + e^- \rightarrow Ag^+$ reactions as separate half reactions, using a recently developed grand canonical extension of the Car−Parrinello method.[13] Of particular interest are the relaxation (Franck−Condon) energies, which, as we will show, are on the order of electronvolts. The results for the energetics will be validated by a computation of the reaction free energy (redox potential) of the total reaction

$$Ag^{2+} + Cu^+ \rightarrow Ag^+ + Cu^{2+} \qquad (1)$$

Bulk solvent conditions can also directly alter the electronic structure of transition metal complexes, smearing out the orbitals over solvent molecules beyond the ligands in the first solvation shell. This raises questions regarding the position of the energy levels of the solute relative to the solvent. In the one-electron picture of ligand field theory, many of the special properties of transition metal aqua ions, such as open valence shells, depend on the condition that the d-levels of the central metal atom/ion are higher in energy as compared to the occupied orbitals of its ligands. Is this also true for the orbitals of molecules in the second solvation shell and further out in the bulk solvent? The density functional theory (DFT) framework used here is particularly suitable to answer this question, and thus, in addition to total energies, we have also computed the one-electron density of states for our four model ions.

Whereas one-electron energy levels cannot be directly observed, they are the main ingredients of electronic absorption spectra. Accordingly, some of the key features of the energy level scheme of the Ag^+ and Cu^+ aqua ions will be verified by computation of the UV spectrum using time-dependent density functional perturbation methods.[14] The optical spectra of the monocations are also of interest because they are a very sensitive probe of solvent fluctuations. This is because d → s transitions are strongly forbidden in high-symmetry environments and the intensity is borrowed from coupling to the solvent.

Ab Initio Molecular Dynamics Method

The fast solvation dynamics makes aqua ions of Cu and Ag ideal model systems for the application of the method of density functional-based ab initio molecular dynamics (Car−Parrinello),[15] and a number of studies have already appeared in the literature. Analyzing a 16 ps molecular dynamics (MD) trajectory of aqueous Cu^{2+}, Pasquarello et al.[16] were able to give a detailed picture of the rapid exchange of equatorial and axial ligands. These fast pseudo rotations act in conjunction with the Jahn−Teller effect, which by elongating the metal oxygen distances along an octahedral axis facilitates replacement of the axial ligands. The Ag^+ aqua ion was investigated in ref 17. In agreement with experiment, the hydration shell was found to consist of four H_2O molecules in continuous motion. Ab initio MD has also proven to be very useful for elucidating structure and dynamics of two further "household" aqueous ions, the hydronium (H_3O^+)[18,19] and hydroxyl ions (HO^-).[20]

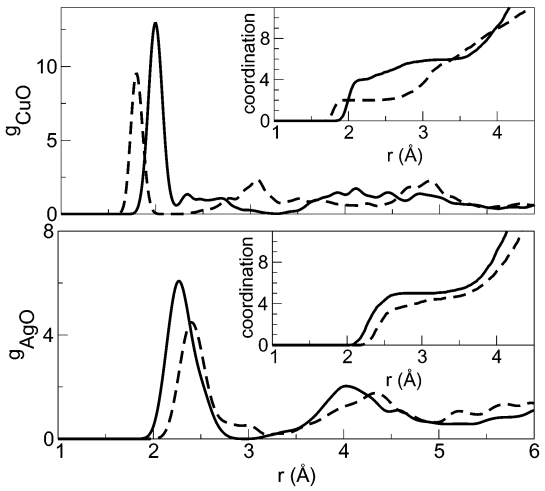

Figure 1. Ion−solvent pair correlations for copper (top) and silver (bottom) aqua ions. The oxygen−metal radial distribution functions $g(r)$ (RDF) are drawn in dashed lines for Cu^+ and Ag^+ and in solid lines for Cu^{2+} and Ag^{2+}. The insets show spherical integrals of the RDF indicating the coordination numbers. Note the anomalously small radius for Cu^+.

The technical specifications of the present density functional calculations are similar to those in ref 17. The calculations are based on the BLYP functional[21,22] and are implemented using a plane-wave basis set and norm conserving pseudo potentials. The study of the redox reactions included spin polarization, while the optical absorption of the monocations was computed from a trajectory generated using a spin restricted scheme. Pseudo-potential parameters and further technical details are summarized in the Appendix. The calculations were carried out using the CPMD code.[23] We have investigated four solvent model systems consisting of 16, 32, 50, and 128 H_2O molecules and a single metal ion in a simple cubic periodic MD cell. The solvent density was set to the ambient density of the pure solvent in each system. For the 32 H_2O system, this leads to a cubic box of 9.86 Å (this choice of solvent density is justified in ref 17).

Structure and Solvation

Radial Distribution Functions. The key structural result is given in Figure 1, showing the metal−oxygen radial distribution functions (RDF). Cu^{2+} is observed to fluctuate between tetragonally distorted octahedral, square pyramidal, and trigonal bipyramidal coordination. The average metal−oxygen distance as defined by the position of the first maximum in the RDF is 2.0 Å. In the octahedral coordination, the axial ligands are elongated (Jahn−Teller distortion) and exhibit large amplitude motions. The coordination number of Cu^{2+} is 5.7, lying between the traditionally accepted six-fold coordination[1,24] and recent results suggesting five-fold coordination.[16,25]

The hydration of Ag^{2+} is similar and at least as dynamical but with a significantly larger radius of 2.25 Å. Upon reduction,

(13) Tavernelli, I.; Vuilleumier, R.; Sprik, M. *Phys. Rev. Lett.* **2002**, *88*, 213002.
(14) Hutter, J. *J. Chem. Phys.* **2003**, *118*, 3928.
(15) Car, R.; Parrinello, M. *Phys. Rev. Lett.* **1985**, *55*, 2471.
(16) Pasquarello, A.; Petri, I.; Salmon, P. S.; Parisel, O.; Car, R.; Tóth, Powell, D. H.; Fischer, H. E.; Helm, L.; Merbach, A. E. *Science* **2001**, *291*, 856.
(17) Vuilleumier, R.; Sprik, M. *J. Chem. Phys.* **2001**, *115*, 3454.
(18) Marx, D.; Tuckerman, M. E.; Hutter, J.; Parrinello, M. *Nature* **1999**, *397*, 601.
(19) Geissler, P.; Dellago, C.; Chandler, D.; Hutter, J.; Parrinello, M. *Science* **2001**, *291*, 2121.
(20) Tuckerman, M. E.; Marx, D.; Parrinello, M. *Nature* **2002**, *417*, 925.
(21) Becke, A. D. *Phys. Rev. A* **1988**, *38*, 3098.
(22) Lee, C.; Yang, W.; Parr, R. *Phys. Rev. B* **1988**, *37*, 785.
(23) Hutter, J.; Parrinello, M. Car−Parrinello Code (CPMD) developed by J. Hutter and the group of numerical intensive computing at IBM Zurich Research Laboratory and the group of M. Parrinello at MPI in Stuttgart.

the ionic radius of the silver cation increases from 2.25 to 2.35 Å, consistent with the loss of electrostatic binding energy of Ag^+ relative to Ag^{2+}. Simultaneously one molecule is expelled from the first hydration shell and the coordination number is lowered from 5 to 4. The radius of the first hydration sphere of aqueous Ag^+ and the corresponding coordination number are in the range of experimental data[3,4,6] (2.31−2.48 Å, respectively, for 2−4 water molecules).

A Cu^+ aqua ion, created by vertical reduction of Cu^{2+}, undergoes a more drastic reorganization than does Ag^+. Instead of expanding, the ionic radius shrinks to 1.8 Å, and the coordination is reduced to 2 with a variable number of molecules at larger distances. Linear coordination of d^{10} ions can be viewed as a result of σds hybridization or a second-order Jahn−Teller effect.[12] Mixing of the *n*d HOMO ($n = 3, 4$) with the empty ($n + 1$)s orbital enables the antibonding d orbital to move the charge from the lobe pointing at the ligand to the perpendicular lobe. This reduces the Pauli repulsion and allows the ligand to come closer, gaining electrostatic attraction energy.[7,8] In solid compounds of Ag^+, this deformation is manifested in a certain preference for chainlike structures with two-fold coordination.[1] In the gas phase, it leads to a marked discontinuity in the stepwise formation constant of $Cu^+(H_2O)_n$ complexes when *n* is increased from 2 to 3.[7−11] A qualitatively similar decrease in the differential hydration energy is observed for $Ag^+(H_2O)_n$, but the size of the discontinuity is much smaller as compared to gas-phase copper hydrates. The difference between the IB ions is enhanced in solution, where, according to our calculations, the tendency to two-fold coordination persists for Cu^+, whereas Ag^+ prefers coordination by four approximately equivalent water molecules. The contrast between the Cu^+ and Ag^+ aqua ions is a striking illustration of the susceptibility of the aqueous solvent to differences in ionic radius. Evidently, because of the larger ionic radius of Ag^+, the electrostatic energy gained by pulling in two solvent molecules is not sufficient to compensate for the loss in energy of the other ligands which are pushed away.

Charge Density. The interaction with the two tightly coordinated water molecules on opposite sides of the ion changes its shape from a sphere to an oblate ellipsoid. The deformation is visualized in Figure 2, showing the difference of the electronic density of an instantaneous configuration of the hydration complex relative to a superposition of densities of free molecules and ions. The accumulation of negative charge protruding sideways perpendicular to the axis of the Cu^+ dihydrate is large enough to occasionally turn around a water molecule in the second solvation shell and form a hydrogen bond with the H atom of this molecule, as is the case in Figure 2.

To quantify the anisotropy of the Cu^+ charge distribution, we have computed the average eigenvalues of the quadrupolar tensor. The electronic density was obtained using the maximally localized Wannier function method.[26] Application of this method gives five Wannier functions localized at or very near to the position of the nucleus with the nodal structure of the d-functions. A similar technique was used by Silvestrelli and Parrinello in ref 27 to compute the effective dipole moment of a water molecule in the liquid (see also ref 28). The results are quadrupole moments (with respect to the center of charge) of $\Theta_{xx} = +2.9$, $\Theta_{yy} = -1.2$, $\Theta_{zz} = -1.7 \times 10^{-26}$ esu cm^2, which are comparable in magnitude to the (experimental) quadrupole moments of a gas-phase H_2O molecule, $\Theta_{xx} = -2.50$, $\Theta_{yy} = 2.63$, $\Theta_{zz} = -0.13 \times 10^{-26}$ esu cm^2.[29]

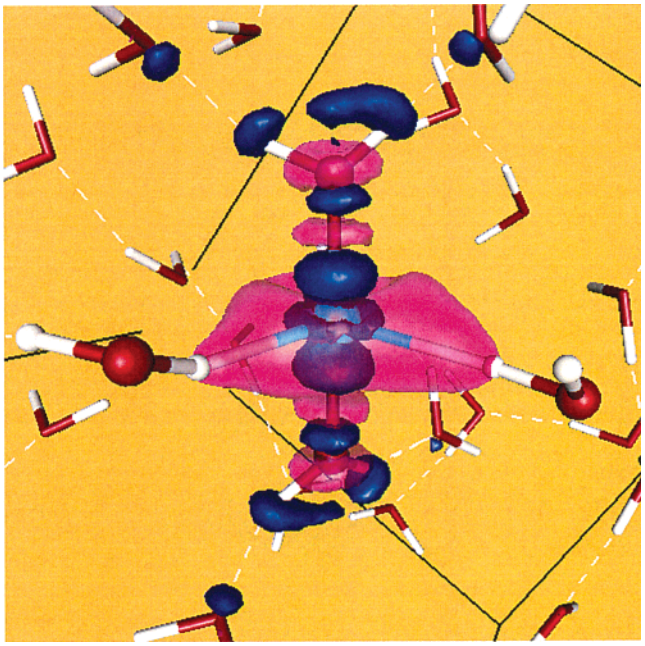

Figure 2. Electron density difference of the aqueous Cu^+ complex visualizing the charge rearrangements with respect to the free ion and molecule species. The Cu^+ ion (light blue) is in the center of the picture. Coordination bonds to solvent molecules are highlighted as cylinders. The pink isosurface indicates an increase in electron density of 0.01 au^{-3}, and the blue isosurface indicates a depletion of −0.01 au^{-3}. The accumulation of electron density perpendicular to the O−Cu−O axis leads occasionally to Cu^+−H bonding as illustrated in this snapshot.

System Size Dependence of Structure. System size is a critical parameter in ab initio MD. The results presented in Figures 1 and 2 were computed using the 32 H_2O model system. Increasing the number of solvent molecules to 50 and 128 was found to have only a minor effect on radial distributions. We therefore conclude that 32 water molecules in a cubic box is adequate for modeling the structure of the first and second solvation shell. This is partly the consequence of the absence of a real counterion, which would severely perturb the solvent structure in such small systems. Charge neutrality is imposed by a homogeneous background of negative charge automatically created by the reciprocal space (Ewald summation) technique used to treat the long-range forces.[30] While artificial, this uniform "counterion" is a better approximation to the high dilution limit than a real ion. For a discussion of size dependence of the energetics, see below and the Appendix.

Comparison to Mixed Quantum Methods. Our prediction for the structure of the Cu^+ aqua ion is somewhat unconventional, and, as direct verification to experiment is not possible, a comparison to the results of other computational investigations

(24) Schwenk, C. F.; Rode, B. M. *ChemPhysChem* **2003**, *4*, 931.
(25) Benfatto, M.; D'Angelo, P.; Della Longa, S.; Pavel, N. V. *Phys. Rev. B* **2002**, *65*, 174205.
(26) Marzari, N.; Vanderbilt, D. *Phys. Rev. B* **1997**, *57*, 12847.
(27) Silvestrelli, P.; Parrinello, M. *J. Chem. Phys.* **1999**, *111*, 3572.
(28) Aguado, A.; Bernasconi, L.; Jahn, S.; Madden, P. A. *Faraday Discuss.* **2003**, *124*, 171.
(29) Verhoeven, J.; Dynamus, A. *J. Chem. Phys.***1970**, *52*, 3222.
(30) Marx, D.; Hutter, J. Ab Initio Molecular Dynamics: Theory and Implementation. In *Modern Methods and Algorithms of Quantum Chemistry*, proceedings, 2nd ed.; Grotendorst, J., Ed.; NIC Series; John von Neumann Institute for Computing: Jülich, 2000; Vol. 3, pp 329−477.

of the aqueous Cu and Ag monocation may be of interest. Starting with the Ag^+ aqua ion, the geometry obtained by the ab initio MD is in good agreement with the structure of ref 31 computed for the four-fold coordinated ion coupled to a self-consistent reaction field. Our Ag^+ structures, however, are rather different from the results of a recent QM/MM simulation by Rode and co-workers.[32] In this study, the first solvation shell of Ag^+ is treated quantum mechanically, leading to a preference of five- and six-fold coordination. It would be interesting to see, therefore, if inclusion of the second solvation shell in the QM region gives results in closer agreement to our work, ref 31, and experimental data.[3−6]

Rode and co-workers[33] have also investigated the Cu^+ aqua ion in a classical simulation study using a pair potential for the interaction of the water ligands with Cu^+ based on SCF calculations.[33] They find a six-fold coordination with a Cu−O distance of 2.20 Å, which is certainly a less unusual hydration structure for a closed shell monocation than the dihydrate obtained by the ab initio MD. However, the SCF calculations of ref 33 are inconsistent with the marked discontinuity of binding energies of water ligands characteristic for the Cu^+ ion. The observed pronounced coordination number dependence of binding energies suggests that many-body effects are essential for the modeling of aqueous Cu^+. Furthermore, the computation of hydration energies of IB ions is very sensitive to the level of treatment of electronic correlation as pointed out in refs 7 and 10. Neglect of these effects could be part of the reason the SCF derived pair potential used in ref 33 leads to coordination numbers in solution that are significantly higher than those obtained in this work.

Computation of the Redox Potential

Two-Surface Method. Can the different redox potentials of the Ag/Cu half reactions be related to the structural differences of the aqua ion complexes as found in the MD simulation (Figure 1)? Before we can address this question, we must verify that our results are consistent with the −1.8 eV thermodynamic driving force of reaction eq 1 as observed in experiment. Because the calculations were carried out in periodic cells containing a single ion at variable oxidation state, we are required to show that the free energies of the corresponding half reactions add up to the free energy of the total reaction eq 1. Here, the "one-component solution model" underlying our method has a distinct technical advantage: Changes in the number of electrons can be instantly compensated. This is the simple idea behind the grand-canonical extension of the ab initio MD method developed in ref 13 for the simulation of redox half reactions. The metal ion + solvent system contained in the "computational" half cell is free to exchange electrons with a fictitious electron reservoir of fixed chemical potential μ. The reservoir can substitute for real metal electrodes in electrochemical cells, because for the type of redox reactions considered, with both reactant and product ions remaining in solution, the electrodes act as a catalyst. The thermodynamic driving force, measured as a potential difference between the electrodes, should be in principle the same for different electrodes.

The grand canonical method introduced in ref 13 is, in essence, a two-surface simulation of a system of N atoms: One potential energy surface (PES) is the electronic ground-state energy $E_R(\mathbf{R}^N)$ of the reduced system R for given atomic positions $\mathbf{R}^N$, and the second PES is the ground-state energy $E_O(\mathbf{R}^N)$ of the oxidized system O with one electron less at the same nuclear configuration $\mathbf{R}^N$. Note that $E_M(\mathbf{R}^N)$ represents the total energy of the full system M. Thus, in the present application, R is the monocation + solvent and O is the dication + solvent. The system switches between these two surfaces depending on how the vertical ionization energy

$$\Delta E(\mathbf{R}^N) = E_O(\mathbf{R}^N) - E_R(\mathbf{R}^N) \tag{2}$$

compares to the applied electronic chemical potential μ: If $\Delta E \geq -\mu$, the ionic forces are computed from the reduced PES; if $\Delta E < -\mu$, they are computed from the oxidized surface. The net effect on the ion dynamics is that of a composite potential energy surface given by

$$E_\mu(\mathbf{R}^N) = \min[E_R(\mathbf{R}^N), E_O(\mathbf{R}^N) + \mu] \tag{3}$$

The proof that the PES of eq 3 is the proper effective ionic potential for an open (grand canonical) electronic system in the limit of zero electronic temperature is given in ref 13 and follows the argument in Chapter 4 of ref 34. Reference 13 also gives the expression for the force on the ions and technical details concerning the implementation in ab initio MD. The surface crossing method introduced here can be compared to a number of other methods in computational physical chemistry. A short discussion of some of these parallels and distinctions, which could be helpful in clarifying the strength and limitations of our method, can be found in the Appendix.

Numerical Titration Method. Equation 3 has a rather straightforward interpretation, which is illustrated in Figure 3. Electronic chemical potentials in the condensed phase are negative. As a result, adding a bias μ lowers the PES of the oxidized state with respect to the PES of the reduced state. Hence, while E_O normally lies above E_R (vertical ionization potentials are positive), for sufficiently negative μ the surfaces will intersect, creating a region in configuration space where the oxidized system is stable. Lowering μ further closes the energy gap between the minima in the two basins of stability for R and O, and the potential E_μ of eq 3 will develop into a double well potential (as a function of a suitable reaction coordinate). The stable configurations will be in general different, and R and O can expected to be separated by a sizable activation barrier.

The potential energy picture sketched in Figure 3 suggests that the value of μ at which the O and R minima become degenerate is special. In the zero temperature limit, it is equal to the adiabatic ionization energy, and, hence, it can be used as a rough estimate of the redox potential. This relationship carries over to free energies at finite (ionic) temperature and can be made rigorous. In ref 13, it is shown that at a given temperature T the particular value of $\mu := \mu_{1/2}$ for which both oxidation states are equally probable can be identified with the free energy difference $\Delta A(T)$ between R and O:

$$\Delta A = A_R - A_O = \mu_{1/2} \tag{4}$$

(31) Martinez, J. M.; Pappalardo, R. R.; Sánchez Marcos, E. *J. Phys. Chem. A* **1997**, *101*, 4444.
(32) Armunanto, R.; Schwenk, C. F.; Rode, B. M. *J. Phys. Chem. A* **2003**, *107*, 3132.
(33) Pranowo, H. D.; Bambang Setiaji, A. H.; Rode, B. M. *J. Phys. Chem. A* **1999**, *103*, 11115.

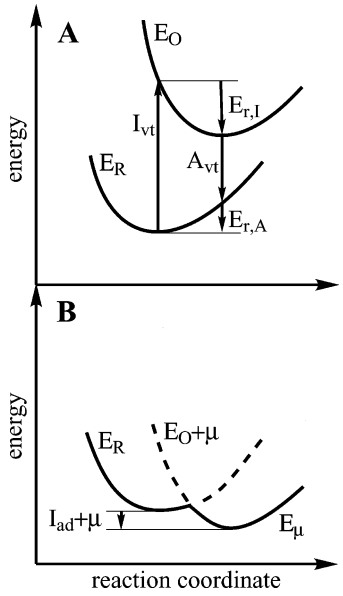

Figure 3. Schematic diagram showing the potential energy surface (PES) E_M of a reduced (M = R) and oxidized (M = O) system as a function of a reaction coordinate describing the change in solvent structure during oxidation. Shown is a closed system (A) and an open system (B) which can exchange electrons with a reservoir at fixed electronic chemical potential μ. I_{vt} is the vertical ionization energy of state R, and A_{vt} is the vertical electron affinity of state O. $E_{r,I}$ and $E_{r,A}$ are the relaxation (Franck−Condon) energies which make up the difference between I_{vt} and A_{vt}. The adiabatic ionization energy I_{ad} is defined as $I_{vt} + E_{r,I}$. Negative chemical potentials μ decrease the energy gap (as illustrated in B), allowing the PESs of the oxidation states to cross. The solid curve in B corresponds to the minimum PES E_μ (see eq 3) governing the dynamics of the open system.

with the (Helmholtz) free energy derived from the partition function for each single PES E_M, M = R, O, according to

$$A_M = -k_B T \ln \Lambda^{-3N} \int d\mathbf{R}^N \, e^{-E_M(\mathbf{R}^N)/k_B T} \qquad (5)$$

Λ in eq 5 is the average thermal wavelength defined as $\Lambda^{-3N} = \prod_j \lambda_j^{-3N_j}/N_j!$, where λ_j is the thermal wavelength $\lambda_j = h/\sqrt{2\pi m_j k_B T}$ of the N_j nuclei of species j, and N is the total number of nuclei.

The electronic chemical potential of the reservoir is an external parameter under our control. We can, therefore, determine $\mu_{1/2}$ by varying μ until the system is observed to spend equal amounts of time in the reduced and oxidized state, giving us according to eq 4 an estimate of the reaction free energy. In practice, this means a search for the value of μ where the system changes over from being predominantly in the R state to the O state or vice versa. This produces a σ-shaped variation of the number of electrons (oxidation state) with the chemical potential which can be compared to the titration curves for the determination of acid dissociation constants (pK_a). The "numerical titration" method described above was applied to the $Cu^{2+} + e^- \rightarrow Cu^+$ and $Ag^{2+} + e^- \rightarrow Ag^+$ half reactions. Two chemical potential sweeps were performed for each species, one with decreasing and one with increasing values of μ using again the 32 solvent molecule system. The response of the system is shown in Figure 4. The MD runs at fixed μ had a duration between 2 and 3 ps. This time is in general too short to reach chemical equilibrium. As a result, oxidation in the downward

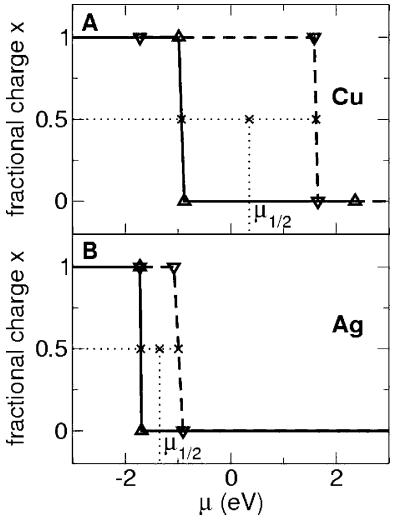

Figure 4. Oxidation state of a model aqueous solution of Cu (A) and Ag (B) ions as a function of the applied electronic chemical potential μ. The ionic solution is in the oxidized state M^{2+} (M = Ag, Cu) if $x = 1$ and in the reduced state M^+ if $x = 0$. A stepwise decrease of μ (solid lines with triangles pointing upward) converts M^+ into M^{2+}. Because of the barrier separating the product and reactant (see Figure 3), the reverse reaction in the upward μ sweep (dashed lines with triangles pointing downward) occurs at higher values of μ. The value $\mu(x = 0.5) := \mu_{1/2}$ is taken to be in the middle of the loop and is used as an estimate of the reaction free energy ΔA (see eq 4). Due to the interaction with periodic image charges and neutralizing background charge, only relative values of $\mu_{1/2}$ can be compared to the experiment.

sweep occurs at lower values of μ than reduction in the upward sweep. The hysteresis is caused by the energy barrier separating the R and O state (Figure 3), and the width of the loop will be larger the more difficult it is to cross this barrier. The hysteresis for the Cu^+ oxidation in Figure 4 is wider than that for Ag^+ because the reconstruction of the solvation shell of the Cu aqua ion is so much more severe. Taking the center of the hysteresis in Figure 4 as an estimate for $\mu_{1/2}$ and subtracting the values ΔA_M of the two half reactions, M = Cu, Ag, we obtain a redox free energy $\Delta\Delta A = \Delta A_{Ag} - \Delta A_{Cu} = -1.7$ eV for the full redox reaction eq 1. This number compares very well to the experimental free enthalpy of −1.8 eV. The value of the free energy computed for the Ag half reaction was confirmed by an alternative approach using thermodynamic integration.[35]

System Size Dependence of Redox Potential. The electrostatic interactions between ions, their periodic images, and the homogeneous background in our small ab initio MD model systems are on the order of electronvolts. The system size dependence of the absolute reaction free energies ΔA is indeed extreme, judging from the 5−6 eV difference between the $-\mu_{1/2}$ values in Figure 4 and the experimental free enthalpies of oxidation ΔG_{ox} at infinite dilution given in Figure 5. The good agreement of $\Delta\Delta A$ with experiment is therefore somewhat surprising and must be attributed to a rather fortunate cancellation of errors. The reason is that the long-range interactions are very similar for the two half reactions studied here and hence, to a very good approximation, cancel out. We tested this hypothesis by comparing the relative reaction energy $\Delta\Delta E$ of the Ag and Cu half reactions obtained in the 32 H_2O model to the result for a 50 molecule system. The numbers we found, $\Delta\Delta E = -2.13$ and -2.10 eV, respectively, are indistinguishable and reasonably close to the experimental enthalpy difference

(34) Parr, R. G.; Yang, W. *Density-Functional Theory of Atoms and Molecules*; Oxford University Press: New York, 1989.

(35) Blumberger, J.; Sprik, M. *J. Phys. Chem. B*, in press.

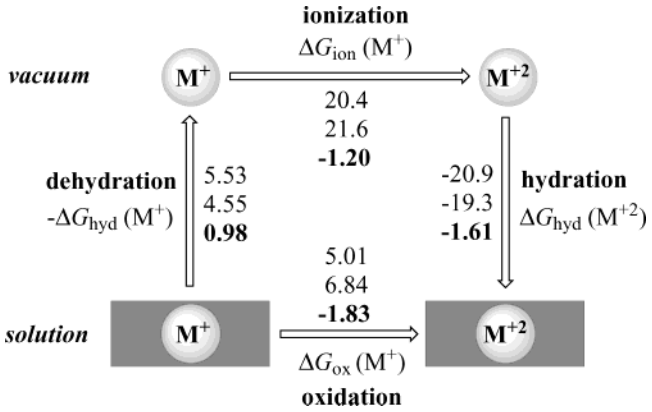

Figure 5. Thermodynamic (Born−Haber) cycle for the oxidation of the IB aqua ions $M^+ = Cu^+$ and Ag^+ from experimental thermodynamic data. Energies are given in electronvolts and correspond (from top to bottom) to Cu, Ag, and the difference between Cu and Ag. The free hydration enthalpies ΔG_{hyd} are standard absolute values in the limit of infinite dilution calculated from experimental relative free formation enthalpies (ref 54) using the estimated absolute free hydration enthalpy of aqueous H^+ of ref 55.

of −1.76 eV at infinite dilution (a more detailed analysis of size effects will be given in the Appendix and ref 36).

Energetics

Thermochemical Picture. Normally the value of electrode potentials is rationalized in terms of a thermodynamic cycle. Oxidation of a metal cation is viewed as a succession of three steps: transfer to vacuum (dehydration), ionization in a vacuum, and resolvation of the product. For the Cu and Ag aqua ions, the thermochemical constants of these three reactions are known and summarized in Figure 5. In this Born−Haber picture, a substantial fraction of the 1.8 eV of the Cu/Ag couple is due to the gas-phase ionization energy of Ag^+, which is 1.2 eV higher as compared to Cu^+. The remaining 0.6 eV is accounted for by the favorable enthalpy of hydration of Cu^{2+}. This advantage in solvation energy of the dication is clearly the result of the smaller ionic radius of Cu^{2+} as compared to that of Ag^{2+}. However, also the big difference in the vacuum ionization potential is ultimately related to the difference in size. Because of the more diffuse character of the 4d shell of Ag, screening is less effective in comparison to the 3d shell of Cu, and the cost of removing an electron is therefore higher.

Energy Relaxation Picture. It is instructive to view the reaction from the perspective of oxidation taking place entirely in solution, that is, as a combination of vertical ionization and relaxation (Franck−Condon picture). Such a decomposition is inherent in the two-surface grand canonical simulation method and is therefore the natural point of view in this approach. As the reconstruction of the solvation shells involves changes in coordination number (an inner sphere process in the terminology of electron transfer theory), relaxation will substantially reduce the value of adiabatic ionization energies with respect to the vertical ionization energies. The same effect will lead to major discrepancies between the vertical ionization potential of the monocation and vertical electron affinity of the dication (see Figure 3). Because these quantities are identical for metal ions in a vacuum, the large mismatch in solution is perhaps the best illustration of the importance of solvent effects.

(36) Blumberger, J.; Tavernelli, I.; Sprik, M., manuscript in preparation.

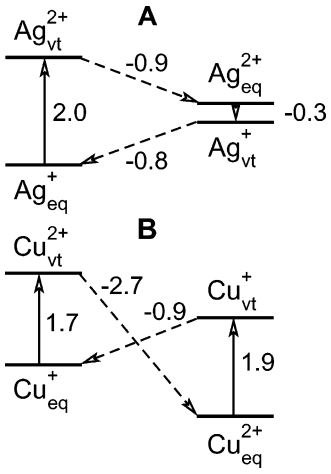

Figure 6. Thermodynamic (Franck−Condon) cycle for the oxidation of aqueous Ag^+ (A) and aqueous Cu^+ (B). The energy levels of M_{eq}^+ and M_{eq}^{2+} (M = Ag, Cu) give the average potential energy along an equilibrium trajectory of length 2−3 ps at 300 K. The model system consists of a periodically replicated cell containing one metal ion + 32 water molecules. The energies indicated by M_{vt}^{2+} and M_{vt}^+ were obtained by adding the vertical ionization potential to the total energy of M_{eq}^+, respectively, subtracting the vertical electron affinity from the total energy of M_{eq}^{2+}. Dashed lines represent relaxation energies (compare to Figure 3). The interaction energy of the charged solution with the neutralizing background is included in the energy levels. All energy values are given in electronvolts.

All of this information is summarized in Figure 6, where we compare the total energies in a full redox cycle of a metal ion (oxidation followed by reduction). The energy gap ΔE between the oxidized and the reduced state in Figure 6 is computed as the thermal average of the vertical ionization energy $\Delta E(\mathbf{R}^N)$ of eq 2 and has a different value and interpretation depending on which oxidation state defines the equilibrium. If the solvent is coupled to the reduced PES, ΔE represents the average vertical ionization potential of M^+, whereas ΔE is equal to the vertical electron affinity of M^{2+} when the solution is in the oxidized state.

Going around the redox loop of Ag, starting with equilibrium Ag^+, we see that vertical ionization costs 2.0 eV, with 0.9 eV of energy reclaimed by the relaxation of the solvation shell, which as we saw in Figure 1 consists of the addition of one ligand molecule. Vertical reduction of Ag^{2+} only gains 0.3 eV. The subsequent restoration of the Ag^+ hydration shell releases another 0.8 eV, bringing us back to equilibrium Ag^+. The cycle for Cu is strikingly different. While the vertical ionization energy of the monocation is comparable, the energy produced by the resolvation of the Cu^{2+} is 2.7 eV, a factor of 3 larger than that for Ag^{2+}. The large increase in relaxation energy of Cu^{2+} is due to the drastic reconstruction of its solvation shell, which has to change from the compact dihydrate structure of Cu^+ into a 5−6 molecule shell for Cu^{2+}.

The picture of the energy balance emerging from Figure 6 is rather different from the Born−Haber cycle of Figure 5. Contrary to ionization in a vacuum, the vertical redox reaction in solution is endothermic by as much as 1.7−0.3 = 1.4 eV. This is even opposite to the direction of the $Ag^{2+} + Cu^+ \rightarrow Ag^+ + Cu^{2+}$ reaction. The driving force in Figure 6 is therefore entirely supplied by the huge combined relaxation energy of 2.7 + 0.8 = 3.5 eV, resulting in a net energy change of $\Delta E = -2.1$ eV. Experiment gives for the reaction enthalpy $\Delta H = -1.76$ eV. Comparing the reaction free energy of $\Delta\Delta A = -1.7$

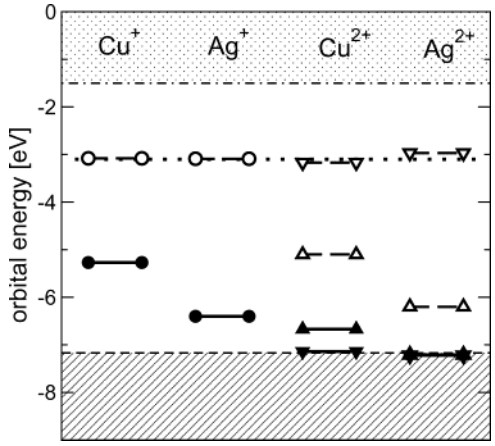

Figure 7. Energy level diagram of aqueous Cu and Ag ion solutions. Filled and open symbols are the highest molecular orbital (HOMO) and lowest unoccupied orbital (LUMO) energies, respectively, averaged over time. For the d^9 ions Cu^{2+} and Ag^{2+}, the minority spin−orbital energies are indicated by triangles pointing upward, and the energies of the majority spin−orbitals are indicated by triangles pointing downward. The redox active states are found in the gap between the valence band (hatched) and the conduction band (dots) of pure water (the thick dotted line marks the energy of the semilocalized LUMO).

eV computed from the response to variation of the chemical potential to the $\Delta G = -1.83$ eV of experiment (see Figure 5), we conclude that both the reaction enthalpy and the entropy are overestimated in our calculation, with the errors largely canceling in the reaction free energy.

Finally, we again express a word of caution regarding size effects. The energies in Figure 6 were obtained using the 32 H_2O model. Vertical ionization energies are subject to similar system size effects as discussed in the previous section for the reaction free energies of half reactions. Indeed, an increase of the number of solvent molecules (to 50 and 128) gave an enhancement in vertical ionization energy on the order of an electronvolt or more. As for $\Delta\Delta A$, only relative values, comparing Ag to Cu ions, are meaningful. Thus, the negative value of the electron affinity of Cu^{2+} in Figure 6 (and similarly the positive value of $\mu_{1/2}$ for Cu^{2+} in Figure 4) is a result of the interaction with the background and will change sign for a sufficiently large cell (see also Appendix). Rearrangement of the solvation shell, on the other hand, occurs at fixed charge. Accordingly, the relaxation energies of the half reactions in Figure 6 are more reliable with inaccuracies of ∼0.2 eV. It is therefore an interesting question whether these Franck−Condon energies can be related to observable quantities in, for example, dynamic electrochemical measurements.

Electronic Structure and Spectroscopy

One-Electron States. Staying within the Franck−Condon framework, we can ask the elementary question of where an electron removed by vertical oxidation is coming from, or where it ends up when added to a solution in an oxidized ionic configuration. Chemical intuition suggests this is the metal ion complex and not some solvent molecules elsewhere in the solution. Figure 7 confirms that this elementary piece of chemical common sense is justified. We find that the LUMO of the minority (α) spin in Cu^{2+} and Ag^{2+} solutions is inserted in the liquid water gap. These orbitals accepting the electron are localized on the transition metal coordination complex and closely resemble the corresponding orbitals of a free hydrate complex, as can be seen in Figure 8A. Similarly, the presence of a Cu^+ or Ag^+ ion lifts the HOMO above the upper edge of valence band of the pure solvent. The frontier orbital is again confined to the complex, implying that the energy for (vertical) extraction of electrons from the solution is minimal when taken from the metal ion complex.

In contrast, the LUMOs of Cu^+, Ag^+ and the LUMOs of the majority (β) spin of the dications are distributed over solute and bulk solvent, as is illustrated in Figure 8B for Ag^+. In a vacuum, these species are closed shell with an s orbital as the first empty state. 4s or 5s orbitals strongly overlap with ligand molecules and are therefore forced to merge in bulk solution with the LUMO of the solvent (see Figure 7). Virtual orbitals, detached from the conduction band, have been observed previously in ab initio simulations of liquid water.[37] These semilocalized states are stabilized by regions where the σ^* orbitals are optimally in-phase. In experiment, such orbitals are thought to give rise to a weak tail appended to the conduction band.[38] However, due to the very limited system size, there is room for only one such orbital in our model system.

Electronic Spectroscopy of Monocations. More surprisingly, the mixing of the water LUMO and the metal s orbital has hardly any effect on the energy. Due to this stability of the energy of the LUMO, with partial metal character, the UV spectra of the monocations, consisting of transitions from occupied metal d orbitals to this state, are of special interest. The spectral shift of Ag^+ with respect to the Cu^+ bands can now be used as an estimation of the relative position of the occupied levels of Cu^+ and Ag^+ (Figure 7). We have computed the UV absorption using the time-dependent density functional theory (TDDFT) formalism[39] in the plane-wave pseudo-potential implementation by Hutter.[14,42] A short description of this method can be found in the Appendix.

The result of the TDDFT computation is shown in Figure 9 as compared to the experimental UV absorption for aqueous Ag^+. The triple peak structure for Ag^+ is reasonably well reproduced. Also, the position of the Cu^+ absorption band relative to Ag^+ is consistent with Cu^+ spectra obtained in pulse radiolysis experiments.[40] Unfortunately, the Ag^+ band in Figure 9 also exhibits a significant redshift of 2 eV. Such discrepancies are not uncommon for density functional calculations of band-gaps. A further well-known limitation of the current TDDFT implementation is a serious underestimation of the frequency of charge-transfer excitations.[41,42] In the present calculation, this deficiency is manifested in a band of intense transitions with a strong solvent → solute component. This band overlaps with the high-frequency end of the metal → metal transitions of interest. It is not observed in experiment and has been removed in Figure 9 (more details will be given in ref 43).

The structure of the UV spectrum of Ag^+ can be understood in terms of a small deformation of the tetrahedral solvation shell

(37) Boero, M.; Parrinello, M.; Terakura, K.; Ikeshoji, T.; Liew, C. C. *Phys. Rev. Lett.* **2003**, *90*, 226403.
(38) Bernas, A.; Ferradini, C.; Gerin, J.-P. *J. Photochem. Photobiol., A: Chem.* **1998**, *117*, 171.
(39) Runge, E.; Gross, E. K. U. *Phys. Rev. Lett.* **1984**, *52*, 997.
(40) Ershov, B. G.; Janata, E.; Michaelis, M.; Henglein, A. *J. Phys. Chem.* **1991**, *95*, 8996.
(41) Dreuw, A.; Weisman, J. L.; Head-Gordon, M. *J. Chem. Phys.* **2003**, *119*, 2943.
(42) Bernasconi, L.; Sprik, M.; Hutter, J. *J. Chem. Phys.* **2003**, *119*, 12417.
(43) Bernasconi, L.; Blumberger, J.; Sprik, M.; Vuilleumier, R., manuscript in preparation.

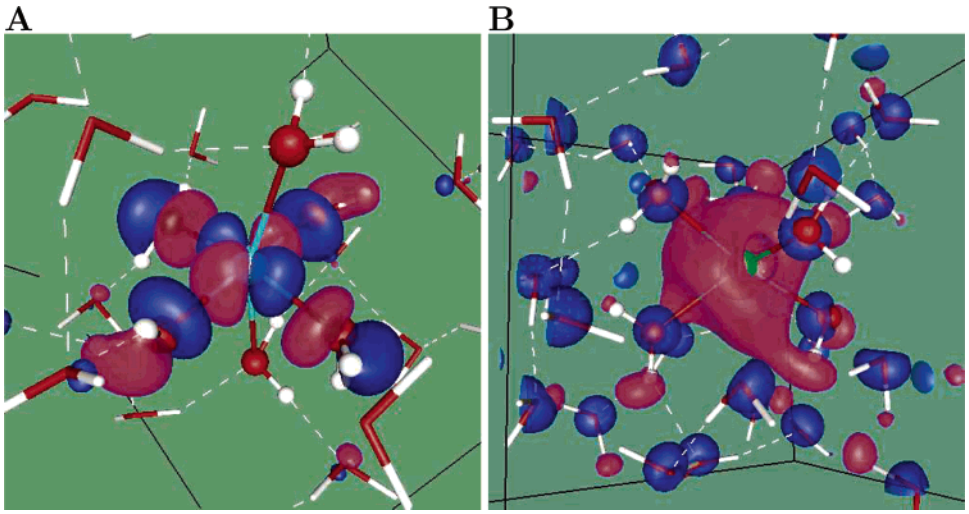

Figure 8. Lowest unoccupied molecular orbital (LUMO) of (A) the minority spin electron in aqueous Cu^{2+} and (B) the Ag^{+} aqua ion. The isosurfaces drawn in pink and blue have opposite signs. The Cu^{2+} LUMO is localized on the coordination complex, whereas the Ag^{+} LUMO is delocalized over the solute (Ag, green sphere in center of the picture) and solvent. For the orbital energies, see the level scheme of Figure 7.

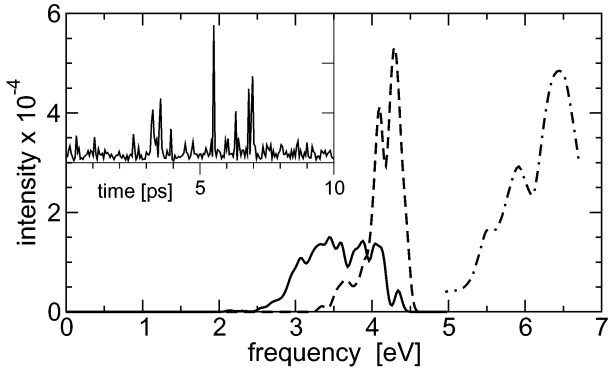

Figure 9. Electronic absorption spectrum of aqueous Ag^{+} (dashed line) and Cu^{+} (solid line). The dashed−dotted line gives the experimental Ag^{+} spectrum.[3] Transient measurements[40] show that the Cu^{+} spectrum is downshifted by 1.3 eV with respect to the Ag^{+} spectrum. The inset shows the adiabatic fluctuations of the sum total of the oscillator strength of the Cu^{+} transitions.

amounting to contraction of the tetrahedron along one of its C_2 axes. Such a static ligand field picture no longer applies to Cu^{+}. As is evident from the inset of Figure 9, the intensity is highly nonuniform in time, showing short bursts of optical activity. Further analysis shows that these events are correlated with the configurations in which one or more of the loosely coordinated solvent molecules has turned around and points a proton toward the Cu ion. The energies of the d orbitals of these "hydrogen-bonded" cations are lower than average. As a result, the high-frequency part of the Cu^{+} spectrum is largely determined by these rare solvent fluctuations. This observation must remain rather hypothetical, because the measurements of ref 40 show little structure, presumably because of low resolution related to the instability of the Cu^{+} ions.

Summary and Outlook

Using a combination of density functional-based computational methods, we have studied the charge +1 and +2 Cu and Ag aqua ions and their mutual redox reaction from various angles. The general picture that emerges is that of two highly dynamical transition metal coordination complexes strongly coupled to the solvent. The focus of the investigation was on the reorganization of the hydration shell in response to vertical oxidation or reduction. For Ag and Cu aqua ions, this process involves changes in coordination number and can, therefore, not be understood without taking the interactions with the surrounding bulk solvent into account. Finite temperature fluctuations of the solvent were also shown to be crucial for the interpretation of the optical spectrum of Cu^{+}. Furthermore, the band structure of the solvent was found to play an important role, effectively confining the redox active states to the energy gap and distributing the s state over a large region in the solution.

A further objective of this study was to analyze the contrast in the redox chemistry of Cu and Ag from the perspective of electrochemical half reactions. The most pronounced manifestation of this difference, ultimately related to the first row character of Cu, was the radically different solvation of Cu^{+} in the form of a compact dihydrate. As a consequence of the short lifetime of aqueous Cu^{+} ions, this theoretical result must remain a prediction, which hopefully can be verified by direct experimental observation. The agreement between our calculations and experiment for the value of the −1.8 eV reaction free energy of the Ag/Cu redox couple can, however, be regarded as indirect evidence for the predicted Cu^{2+} structure, as it allows us to understand the large thermodynamic driving force in terms of a difference in relaxation (Franck−Condon) energy of the $Cu^{2+} + e^{-} \rightarrow Cu^{+}$ half reaction as compared to $Ag^{2+} + e^{-} \rightarrow Ag^{+}$.

The computational methods applied in this study are at the limit of what is currently feasible in density functional calculations. The minimal system dimensions are and will remain a major concern. Finite size effects were minimized as much as possible by using model solutions consisting of just one metal ion + solvent under periodic boundary conditions. Exploiting the fact that the chemical differences between Ag and Cu aqua ions are a short-range effect, depending mainly on interactions with the first and second solvation shell, this model was able to reproduce the experimental redox free energy within an error of 0.1−0.2 eV. It is not unreasonable to believe that this observation is of more general validity and that a similar approach can be extended to the study of other transition metal complexes and small molecules.

Acknowledgment. This research was supported by the EPSRC. We also acknowledge financial support by the Austrian Academy of Sciences (J.B.) and the Swiss National Fund (I.T.). Computing resources were provided by CSE and the HPCx facilities at Daresbury Laboratories. We are grateful for the helpful discussions with Jürg Hutter and Evert Jan Baerends.

Appendix

Ab Initio MD Parameters. The pseudo potentials used in the calculation were constructed according to the Troullier−Martins scheme.[44] For oxygen, the 2s and 2p electrons were included in the valence represented by l = s and l = p components with an equal pseudization radius of $r_c = 1.05$ au. For the H atom, we used a local s potential with $r_c = 0.5$ au. For Cu and Ag, the 3d and 4s, and 4d and 5s electrons, respectively, were treated as valence. The angular momentum channels of Cu (Ag) are 3d (4d), 4s (5s), and 4p (5p) with pseudization radii of 1.3 (1.5), 1.5 (1.8), and 1.5 (2.0) au. The Kleinman−Bylander[45] transformation was used for O, and Gauss−Hermite integration was used for Cu and Ag. The orbitals were expanded in plane waves with a reciprocal cutoff of 70 Ry. The accuracy of these pseudo potentials was tested by comparing the energies and structures of ions and hydrated complexes to the results of all electron calculations carried out with the ADF program.[46] We found that only the computation of the orbital energy of the empty d-level of aqueous Cu^{2+} (Figure 7) requires the use of a semi-core potential with explicit 3s and 3p electrons. We used an analytic 19-electron fully separable pseudo potential according to refs 47 and 48. The fictitious mass of the electrons was set to 700 au, and the MD time step was set to 5 au (0.1209 fs). H atoms have the regular mass of the proton.

Grand Canonical Ab Initio MD Method. For a better understanding of our method for computation of redox potentials, it can be helpful to make a comparison to two well-known methods used in computational chemistry to study systems in states other than ground states. The first method is the Mermin scheme, often applied in the studies of metals. This method is a generalization of the Kohn−Sham method to ensembles at finite electronic temperature. Occupation numbers are now computed from a Fermi−Dirac distribution containing the electronic temperature and chemical potential as parameters (see, for example, ref 34). This method could in principle offer an alternative route for treating systems with variable numbers of electrons. The drawback of this approach is that it generates systems with fractional numbers of electrons, which for molecules with a discrete energy spectrum can lead to serious inaccuracies.[49] These complications are avoided in the two-surface scheme, which works with integer numbers of electrons only.

Dynamics based on a multiple potential energy surface is familiar from studies of excited states. In fact, there is a clear parallel between the grand canonical MD scheme used here and the surface hopping scheme of Tully (for an introduction, see, for example, ref 50). Also, in this method the trajectory crosses over from one potential surface to another. However, there are a number of important differences. Both surfaces in the grand canonical method are stable ground-state energies, the difference being the number of electrons, and can in principle be obtained using standard electronic minimization techniques. Furthermore, the dynamics is strictly adiabatic. Therefore, the dynamics of the surface crossing, currently implemented by an abrupt switch to the more stable surface (see eq 3 and ref 13), has no direct relationship to the actual kinetics of redox reactions in electrochemical cells.

Time-Dependent DFT Calculation. The computation of the optical absorption spectra is based on time-dependent density functional response theory.[51] In this approach, transition frequencies are obtained as poles of the first-order density response function. As is common in this type of calculations, the adiabatic local density approximation (ALDA)[51] was assumed, which neglects the frequency dependence of the density functional. We made a number of further approximations:[14] Whereas the virtual Kohn−Sham levels entering the perturbation calculation as zero-order approximations were computed using the BLYP one-electron potential generated by the ground-state calculation, the response kernel was treated in the local density approximation. Moreover, the coupled perturbed secular equation was solved in the Tamm−Dancoff approximation.

The oscillator strength is evaluated from an expression for the transition dipole adapted to the periodic boundary conditions. Details of this scheme, which is based on the Berry phase expression for the cell dipole moment as developed in the modern theory of polarization,[52,53] can be found in ref 42 together with an application to the electronic absorption spectrum of aqueous acetone. A more detailed account of the computation of the Ag^+ and Cu^+ spectra will appear in a forthcoming publication.[43]

Finite Size Effects and Error Estimation. Accuracy is in ab initio MD simulation of aqueous solutions a point of major concern because of the small system sizes and the short duration of the trajectories. These two sources of error are closely related, as an increase in system dimensions in general implies further restrictions on the time scale of the run. The tradeoff between system size and run length is intrinsic to ab initio MD simulation and is the price one must pay for the study of systems in the liquid state. The errors in the MD are compounded by limitations to the accuracy of the DFT implementation and the various gradient corrected density functionals applied in ab initio MD in particular. A substantial body of work is available in the literature assessing the performance of density functionals for structure and energetics of hydrated clusters in a vacuum and (to a much lesser extent) in hydrogen-bonded solids. Unfortunately, it is not always possible to transfer these results to liquid water and aqueous solutions for reasons which are not completely understood. Conclusive tests can only be made by costly molecular dynamics runs of the liquid. In this section, we review

(44) Troullier, N.; Martins, J. *Phys. Rev. B* **1991**, *43*, 1993.
(45) Kleinman, L.; Bylander, D. M. *Phys. Rev. Lett.* **1982**, *48*, 1425.
(46) Amsterdam Density Functional package. Contributions by E. J. Baerends and his group at the Vrije Universiteit Amsterdam (The Netherlands) and others.
(47) Goedecker, S.; Teter, M.; Hutter, J. *Phys. Rev. B* **1996**, *54*, 1703.
(48) Hartwigsen, C.; Goedecker, S.; Hutter, J. *Phys. Rev. B* **1998**, *58*, 3641.
(49) Vuilleumier, R.; Sprik, M.; Alavi, A. *J. Mol. Struct. (THEOCHEM)* **2000**, *506*, 343.
(50) Tully, J. C. In *Classical and Quantum Dynamics in Condensed Phase Simulations*; Berne, B. J., Ciccotti, G., Coker, D., Eds.; World Scientific: River Edge, NJ, 1998; p 489.
(51) Casida, M. E. In *Recent Developments and Applications of Modern Density Functional Theory, Theoretical, and Computational Chemistry*; Seminario, J. M., Ed.; Elsevier: Amsterdam, 1996; Vol. 4.
(52) King-Smith, R. D.; Vanderbilt, D. *Phys. Rev. B* **1993**, *47*, 1651.
(53) Resta, R. *Rev. Mod. Phys.* **1994**, *66*, 899.

some of the convergence tests we have carried out and make some pertinent comments. The periodic 1 ion + 32 H_2O molecule model which is the basis for most of the results presented in this work is an optimum compromise between system dimension and time scale given the current performance of hardware. Charge neutrality is restored by a neutralizing homogeneous background charge density $-q/L^3$, where q is the charge of the ion and L is the length of the cubic MD cell. As discussed in the section on the computation of the redox potential, there are good reasons to prefer such a "one-component solution model" over a model with explicit counterions. However, as already indicated, size effects are on the order of electronvolts.

The one-component solution model has a long and somewhat controversial history in computational chemistry. It has been used in electronic structure calculation for the computation of the energy of charged defects in solids.[56] The most frequent application, however, has been in classical simulation for computation of hydration energies of ions in aqueous solution.[57−62] The primary question is how to deal with the interaction of an ion with its periodic images and the background charge. This interaction is attractive and can be estimated by the Madelung energy $-q^2\alpha/2L$ of a simple cubic Wigner crystal of point charges of magnitude q.[56,63] $\alpha = 2.837297$ is the Madelung constant. It will be clear that the $1/L$ dependence makes the convergence toward the infinite dilution limit particularly slow and effectively out of reach of currently accessible system sizes in ab initio MD. One option is to subtract the ion self-interaction from the total energy to accelerate convergence with system size. This approach has been applied with some success in the computation of the energy of charge defects in solids.[56]

For the half reaction $M^{2+} + e^- \rightarrow M^{1+}$, the Wigner self-interaction energy is different in the oxidized and reduced states. Hence, to apply this correction, we must subtract from the reaction energy the difference of the energies of the corresponding Wigner crystals, which amounts to adding a correction term

$$\Delta E_W = \frac{\alpha \Delta q^2}{2L} \tag{6}$$

where for dication reduction considered here $\Delta q^2 = 1^2 - 2^2 = -3$. To assess how a change of size would affect our results for the energetics, we have determined the reaction energies for a system consisting of only 16 solvent molecules and a system with 50 molecules, and we compared these results to the data for the 32 molecule system. The results both before and after addition of ΔE_W of eq 6 are given in Table 1.

The Wigner correction seems to give an improvement in convergence of the reaction energy with system size and better agreement with the experimental reaction enthalpies (also given in Table 1). Note, however, that correction overestimates the reduction energies. The 0.5−1 eV discrepancy is significant and consistent with the results for classical ion hydration. Indeed, analysis of the approach to the infinite dilution limit of charging energies has uncovered the existence of a second $1/L$ contribution related to the interaction of the ion with the solvent in image cells. The water molecules in the cells adjacent to the central cell are oriented to solvate an image ion and are therefore in an unfavorable orientation for interaction with the ion in the central cell. This interaction energy is positive and, as shown by Hummer et al.,[57] is compensated by the negative Wigner ion self-interaction. This, perhaps fortuitously, makes the uncorrected energy in classical models for ion hydration almost insensitive to system size (see also ref 60). While this cancellation is not carried over to the quantum system, a similar $1/L$ ion−solvent term must also be present and is currently under investigation.[36] For the reaction energy $\Delta\Delta E$ of the full redox reaction (eq 1), the Wigner terms of both half reactions cancel. Therefore, one can expect a size dependence of $\Delta\Delta E$ that is much smaller than that for ΔE. Indeed, the reaction energies $\Delta\Delta E = -2.13$ and -2.10 eV for the 32 and 50 water molecule system are indistinguishable and reasonably close to the experimental enthalpy difference of -1.76 eV.

Table 1. Reaction Energy ΔE of the Half Reactions for Reduction of Ag^{2+} and Cu^{2+} Ions Determined from Molecular Dynamics Trajectories of Periodic Model Systems Containing a Single Ion and N Water Molecules[a]

	$Ag^{2+} + e^- \rightarrow Ag^+$		$Cu^{2+} + e^- \rightarrow Cu^+$		$Ag^{2+} + Cu^+ \rightarrow$
N	ΔE	ΔE(corr.)	ΔE	ΔE(corr.)	$Ag^+ + Cu^{2+}$
16	−0.38	−8.21	−0.26	−8.09	−0.12
32	−1.16	−7.37	0.97	−5.25	−2.13
50	−1.86	−7.21	0.24	−5.11	−2.10
exp.		−6.27		−4.51	−1.76

[a] The energies indicated by ΔE(corr.) are the result of adding the correction term eq 6, which removes the interaction of the ions, their periodic images, and neutralizing background using the classical point charge approximation of ref 56. The last column gives the reaction energy $\Delta\Delta E$ of the full redox reaction as obtained by subtracting the energies of the half reactions. The numbers in the row labeled "exp." are the experimental reaction enthalpies determined from data given in refs 54 and 55. Energies are given in electronvolts.

The determination of the free energy differences ΔA from the graphs shown in Figure 4 will be subject to size effects comparable to the enthalpy. In addition, the estimate of free energy suffers from uncertainties as a consequence of the hysteresis. Our simple scheme of determining $\mu_{1/2}$ from the middle of the hysteresis loop, while a natural one, is, of course, questionable. For a rough estimate of the corresponding error in ΔA, we can use the width of the hysteresis loop, which gives $\Delta A = -1.38 \pm 0.35$ eV and $\Delta A = 0.35 \pm 1.28$ eV for Ag and Cu reduction, respectively. This would lead to an uncertainty of ± 1.6 eV in the $\Delta\Delta A = -1.73$ eV estimate for the free energy of reaction eq 1. An error of this magnitude would represent a serious detraction from the apparent agreement with the experimental value of $\Delta\Delta A = -1.83$ eV. However, this number is likely to be an upper limit of the error. This is supported by two observations: First, comparing the experimental free enthalpy to the enthalpy of the reaction (see Table 1), we see that entropy contributes only 0.1 eV. This suggests that the 0.3 eV difference we find between the computed values of $\Delta\Delta A$ and $\Delta\Delta E$ (see Table 1) could be a more realistic estimate of the error in our result. Second, for the Ag half reaction, we have validated the result of ΔA using thermodynamic integration

(54) Wagman, D. D.; Evans, W. H.; Parker, V. B.; Schumm, R. H.; Halow, I.; Bailey, S. M.; Churney, K. L.; Nutall, R. L. *J. Phys. Chem. Ref. Data* **1982**, *11*, 154, 160.
(55) Marcus, Y. *J. Chem. Soc., Faraday Trans.* **1991**, *87*, 2995.
(56) Makov, G.; Payne, M. C. *Phys. Rev. B* **1995**, *51*, 4014.
(57) Hummer, G.; Pratt, L. R.; Garcia, A. E. *J. Phys. Chem.* **1996**, *100*, 1206.
(58) Figuerido, F.; Del Buono, G. S.; Levy, M. L. *J. Phys. Chem. B* **1997**, *101*, 5622.
(59) Lynden-Bell, R. M.; Rasaiah, J. C. *J. Chem. Phys.* **1997**, *107*, 1981.
(60) Bogusz, S.; Cheatham, T. E., III; Brooks, B. R. *J. Chem. Phys.* **1998**, *108*, 7070.
(61) Darden, T.; Pearlman, D.; Pedersen, L. G. *J. Chem. Phys.* **1998**, *109*, 10921.
(62) Hünenberger, P. H.; McCammon, J. A. *J. Chem. Phys.* **1999**, *110*, 1856.
(63) Nijboer, B. R. A.; Ruijgrok, T. W. *J. Stat. Phys.* **1988**, *53*, 361.

techniques.[35] Both approaches give virtually identical results, which confirms that $\mu_{1/2}$ taken at the center of the hysteresis is a reasonable choice. The hysteresis may be reduced by using the grand canonical approach in combination with an enhanced sampling technique such as parallel tampering. Future work will be dedicated to this issue.

A further point of concern is the limited simulation time accessible to our ab initio MD approach and its influence on energetics and structure. The radial distribution functions, potential energies, and free energies discussed in the main text are determined from trajectories of 2−3 ps length. For the computation of the optical spectra of Figure 9, the runs for the monovalent aqua ions Ag^+ and Cu^+ were extended to about 10 ps, which did not give any changes of the metal-O and metal-H radial distribution functions. The potential energy of the aqueous metal ion complexes exhibits slow modes on the picosecond time scale, which give rise to uncertainties of the reaction energy ΔE and relaxation energies on the order of 0.1 eV. An estimate of the absolute errors introduced by the limited simulation time cannot be given but is expected to be significantly lower than the uncertainties due to finite size effects.

Finally, the accuracy of density functionals is perhaps most difficult to quantify in the present context as this source of error is entangled with the uncertainties due to limitations of system size and equilibration time. The first benchmark studies of liquid water[64] used system sizes and run lengths similar to that of the core model studied here (32 H_2O molecules, 2−5 ps) and showed that the BLYP functional (as also applied in this study) gave good agreement with experimental data for structure and dynamics. For an appreciation of the effect of the short equilibration times, it should be mentioned that ab initio MD runs are generally initiated from samples prepared by classical MD simulation using a well-tested empirical force field. Subsequent studies[27,65] extending the duration of the simulation to 10 ps and system dimensions to 64 molecules consolidated the early results. These calculations also established that the self-diffusion coefficient shows a strong size dependence, becoming faster in the larger system. Staying within the same regime of length and time scales and sample preparation methodology, this is the basis on which the present calculation must rely. However, the most recent studies[66,67] pushing the run length well beyond the 10 ps range exploiting the latest in computational technology seem to indicate that BLYP water, given enough time to equilibrate, has a tendency to slow down and become overstructured. These observations, if confirmed, could mean that future DFT-based ab initio MD studies will have to make use of improved density functionals.

JA0390754

(64) Sprik, M.; Hutter, J.; Parrinello, M. *J. Chem. Phys.* **1996**, *105*, 1142.
(65) Izvekov, I.; Voth, G. A. *J. Chem. Phys.* **2002**, *116*, 10372.
(66) Asthagiri, D.; Pratt, L. R.; Kress, J. D. *Phys. Rev. E* **2003**, *68*, 041505.
(67) Grossman, J. C.; Schwegler, E.; Draeger, E. W.; Gygi, F.; Galli, G. *J. Chem. Phys.* **2004**, *120*, 300.